Are Hydrogen Bonds Unique among Weak Interactions in Their Ability to Mediate Electronic Coupling?

Emily Cukier, Sarah Daniels, Eric Vinson, and Robert J. Cave*

Department of Chemistry, Harvey Mudd College, 241 East 12th Street, Claremont, California 91711

Received: June 3, 2002; In Final Form: September 10, 2002

Superexchange effects on the electronic coupling element for electron transfer are investigated using water dimers and atomic donors and acceptors. We compare the electronic coupling elements obtained with H-bonded dimers to those obtained for other water dimer geometries at given donor−acceptor and oxygen−oxygen distances. The H-bonded orientation does not yield significantly different coupling elements from non-H-bonded orientations at a given oxygen−oxygen distance. In addition, the distance dependence of the coupling mediated by H-bonds is not significantly different from that for other dimer geometries. It is found that protonation of the intervening waters has a significant effect on coupling elements for donor/acceptor pairs with low ionization potentials. The implications of these results are discussed for condensed-phase ground- and excited-state electron transfers.

I. Introduction

A wide range of experimental and theoretical results have demonstrated the significant effects that an intervening medium can have on the rate of electron transfer (et) between a donor (D) and acceptor (A).[1−18] In theories of condensed-phase nonadiabatic electron transfer, the rate constant for fixed donor−acceptor separation can be written as[6,9,19−25]

$$k(R_{DA}) = \frac{2\pi}{\hbar}|H_{DA}|^2 FC \qquad (1)$$

where *FC* is the Franck−Condon-weighted density of states and H_{DA} is the electronic coupling element for electron transfer. The electronic coupling element is predominantly responsible for the distance and orientation dependence of the rate, at least at large donor−acceptor separations.

The medium surrounding D and A can affect the rate via electrostatic interactions[19,24] (λ_{outer} in Marcus theory) as well as through specific interactions with D or A that alter the relative energetics of the et process. These effects primarily change the *FC* term in eq 1. A second class of medium effects arises through modification of the electronic interactions between D and A.[9] These have been termed "superexchange" effects, and their impact has been observed in a broad array of experimental and theoretical studies for D and A beyond close contact. Superexchange interactions primarily modify H_{DA}, thus most theoretical work aimed at understanding *electronic* medium effects has focused on changes in the electronic coupling.

McConnell[26] and Halpern and Orgel[27] were among the first to suggest that covalent bonds connecting D and A could give rise to significantly greater electronic coupling than would be observed with vacuum separating D and A. Later work by Beratan, Onuchic, and co-workers,[2,10,13,28−33] Newton and co-workers,[9,34−39] Stuchebruhkov and co-workers,[14,16,17,40−49] Marcus and co-workers,[16,44,50,51] Larsson and co-workers,[52−58] Curtiss and Miller,[59−63] and others[64−73] has elucidated many of the detailed aspects of this medium-induced coupling.

The Pathway Model of Beratan and Onuchic[2,10] has emphasized that electronic medium effects likely arise from a complex interplay between through-space interactions, hydrogen-bond interactions, and covalent interactions. The simple parametrization allowed for the rapid analysis of et in large systems, and its general features have seen ample confirmation in comparisons with experiment.[1,5] One aspect of the Pathway Model that has been particularly fertile is the prediction of the importance of H-bonds in the mediation of the electronic coupling. Beginning with the work of Therien and co-workers,[74] a number of model systems have been designed that specifically investigated the efficacy of H-bonds in mediating the coupling.[75−79] In general, the suggestion of the Pathway Model that a hydrogen bond is "worth" about two covalent bonds in mediating the electronic coupling has been supported.[14,70,75−81]

The question thus arises whether other weak interactions (i.e., van der Waals contacts) might be similarly effective in mediating the electronic coupling. Whereas the H-bond is strong on the scale of non-covalent/ionic interactions, a recent theoretical study has shown that the perturbation of the electron density in ice can be well represented by orthogonalization effects between nearest-neighbor waters.[82] Thus, whatever covalency is present in the water H-bond plays a minor role in determining the electron density for an H-bonded pair. Non-H-bonded water dimers will also exhibit significant electronic interactions (via orthogonalization effects) at distances similar to those observed in H-bonded waters. If this is the case, one might expect comparable effects on the electronic coupling between a donor and acceptor mediated by H-bonded and non-H-bonded close contacts. A number of recent experimental studies have indicated that nonbonded interactions may be better mediators of the coupling than has been thought previously,[4,65,83,84] and detailed analyses of tunneling in proteins also indicate that van der Waals contacts can be important contributors to the dominant pathway for electronic coupling.[14]

The question of the relative efficacy of H-bonds among other weak interactions can thus be cast in two parts. First, at a given

* To whom correspondence should be addressed. E-mail: Robert_Cave@hmc.edu.

10.1021/jp026230c CCC: $22.00
Published on Web 10/25/2002

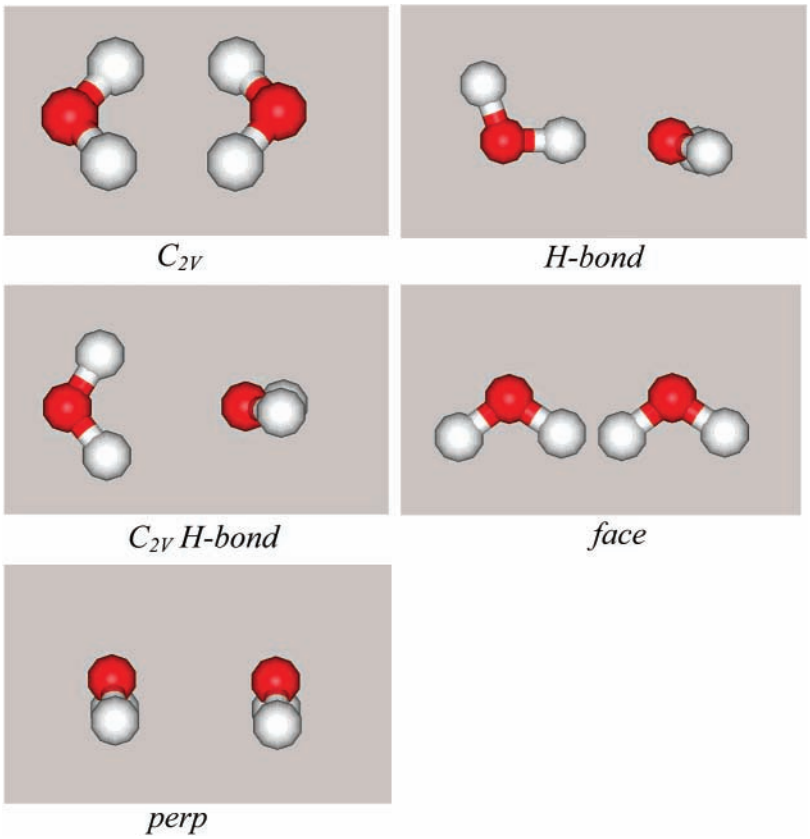

Figure 1. Models of water dimer orientations.

distance between subunits of the bridge/intervening medium, are H-bonded interactions significantly more effective than non-H-bonded interactions at mediating D−A coupling? Second, one can go on to ask whether non-H-bonded interactions at this distance are energetically feasible or long-lived enough to make a significant contribution to the rate. The goal of the present article is to examine the first of these questions. Namely, we compare the electronic coupling mediated by H-bonded and non-H-bonded interactions. Our calculations are based on a model system that has been used previously to study the computational requirements for calculating H_{DA} and the effects of thermally averaged water configurations on the electronic coupling between a donor and an acceptor.[62,66] Whereas our previous studies considered a range of water geometries, neither explicitly considered coupling mediated by the water H-bond. Here, we focus on comparisons with the H-bonded water dimer using two intervening waters in a variety of orientations (see Figure 1) and atomic donors and acceptors (Be, Li). These donors and acceptors minimize orientation effects on the coupling between D/A and water (the initial and final orbitals are s orbitals) and span a significant range of D/A energy relative to the water hole and particle states relevant for et. This simple model system also allows us to use highly correlated wave functions to calculate H_{DA}, which turns out to be important in some orientations of the water dimer.

Our results indicate that the H-bond is not unique among weak interactions in its ability to mediate the electronic coupling for this model system. At a given O−O distance, the coupling for non-H-bonded orientations is comparable to or greater than that for the H-bonded water dimer. The distance dependence of the couplings is similar as well. We also investigate the effects of protonation of the water dimer and find that it has a limited effect on coupling that is likely to be mediated by hole transfer but that it has a sizable effect on particle-transfer-mediated coupling.

II. Theoretical Methods

We examine systems of the type $D-[H_2O]_2-A^+$, with D, A = Be or Li. In a previous study,[62] it was shown that these D/A choices represent a range of ionization potentials of about 4 eV. This study also showed that similar results and conclusions would be obtained if Li were replaced by Na or if Be were replaced by Mg or Zn.

Except where noted, the 6-311++G(d,p) basis[85,86] was used for $Li-[H_2O]_2-Li^+$, $Be-[H_2O]_2-Be^+$, $Li-[H_5O_2^+]-Li^+$, and $Be-[H_5O_2^+]-Be^+$. Test calculations showed that the 6-311G-(d,p) basis[85] underestimated the coupling for $Li-[H_2O]_2-Li^+$ by 20−30% relative to the coupling element calculated with diffuse functions for this system. The dominant contribution to the change in coupling arises from the addition of diffuse functions to the water basis. The $Be-[H_2O]_2-Be^+$ systems were less sensitive to the inclusion of diffuse functions. Test calculations using additional diffuse functions on water (with either Li or Be as D/A) yield less than a 5% change in the coupling relative to the 6-311++G(d,p) values; no conclusions will be affected by these differences. Additional polarization functions had little effect on the coupling in tests with a single intervening water. A test using additional polarization functions with two intervening waters produced less than an 8% change in the coupling compared to the 6-311++G(d,p) basis. Whereas the use of larger basis sets might produce modest effects on the values quoted below, none of our conclusions should be affected. Tests with respect to wavefunction convergence parameters indicate that the H_{DA} values are converged to ±0.00001 eV within a given basis set.

Calculations for Li and Be without waters present used augmented 6-311G(d,p) basis sets having three extra s and p functions, the exponents being obtained by even-tempered extension based on the last two functions in the 6-311G basis set. Further even-tempered extensions produced no significant changes in the coupling for the M_2^+ distances examined here. However, with waters present, use of the 6-311G(d,p) basis for Li and Be was adequate. In part this is because the basis functions on the waters are able to compensate for the inadequate long-range behavior of the Li or Be 6-311G(d,p) basis sets, at least in the region of the waters (a basis set superposition effect). In addition, the decay of the Li- or Be-based orbitals will naturally be modified because of superexchange effects in the region of the waters, and these shape changes are well represented by the water-centered basis functions. These effects have been observed previously by Curtiss and Miller[59,61] for covalently bonded D−A systems.

The electronic coupling element was calculated using the two-state generalized Mulliken−Hush method:[64,87]

$$H_{DA} = \frac{\mu_{12}\Delta E_{12}}{\sqrt{(\Delta\mu_{12})^2 + 4\mu_{12}^2}} \qquad (2)$$

All quantities pertain to the pair of *adiabatic* states associated with the diabatic states of interest; $\Delta\mu_{12}$ is the length of the dipole moment difference vector for the pair of states, μ_{12} is the transition dipole moment (projected on the direction defined by the diagonal dipole moment difference[64,87]), and ΔE_{12} is their energy difference. The method is based on the assumption that the direct contribution to the transition dipole moment from the diabatic states is small because of the weak distance dependence of the dipole moment operator.[64,87] In the current instance, we also assume that the diabatic states of interest are well described by the pair of lowest adiabatic states, although the GMH approach is not inherently limited to the two-state limit.[88] Multistate effects were not explicitly considered in the present studies, in large part because we expect near-degeneracies to be unimportant for these systems, especially for the symmetrical cases.

We compare coupling elements at the idealized geometries discussed below, some of which do not correspond to the transition state for the reaction considered. Past calculations[64,89] indicate that the coupling element is weakly dependent on the energy separation between the adiabatic states (i.e., the Condon approximation is valid). In addition, we find no correlation between adiabatic splitting and the size of the coupling at a fixed donor−acceptor distance, suggesting that deviations from Condon behavior are not a significant factor for these systems.

Since we are concerned with relatively weak interactions, we used correlated wave functions for all states. (In fact, for the perp dimer, uncorrelated results for H_{DA} were significantly smaller than the correlated results.) All energies, dipole moments, and transition dipole moments used as input to the GMH method were calculated using equations of motion (EOM) coupled-cluster methods.[90−95] These methods have been shown to yield highly accurate results for ionization potentials, electron affinities, and electronic excitation energies. In particular, for the calculation of the electronic coupling between Be and Be^+ mediated by two waters, we use the EOM-IP (equations of motion, ionization potential) method. The initial state is a CCSD (coupled-cluster singles and doubles) wave function for Be−$[H_2O]_2$−Be (i.e., a neutral ground state), and annihilation and annihilation + single-excitation operators are applied to the initial state to generate a basis of correlated singly ionized configurations. The two lowest EOM-IP solutions are used to calculate the electronic coupling. For Li_2^+, we used the EOM-EA (equations of motion, electron affinity) method. The initial state corresponds to Li^+−$[H_2O]_2$−Li^+ (i.e., a doubly ionized state), with creation and creation + single-excitation operators applied to generate singly ionized basis states. The two lowest EOM-EA solutions are used in the calculation of H_{DA}. In the protonated dimers, similar schemes are used, with the Be case beginning from a +1 initial state and the Li case beginning from a +3 state. In symmetrical cases, we have been able to compare the energy differences for pairs of states using EOM methods and single-state methods up to CCSD(T) (coupled-cluster singles and doubles with noniterative triple excitations). The latter results should be near full-CI quality for these systems, and the EOM results are at least as good as CCSD energy differences and are frequently quite close to CCSD(T) results.

EOM-CC methods require the solution of a non-Hermitian set of linear equations. The left and right eigenvalues are identical, but the left and right eigenfunctions are different, leading to left and right transition dipole moments that are not Hermitian conjugates. In a two-state system, when the left and right transition dipole moments are collinear, identical values are obtained for H_{DA} by either (i) diagonalizing the non-Hermitian dipole moment matrix, transforming the Hamiltonian matrix with the left and right eigenfunctions, and then calculating the electronic coupling as the geometric mean of the off-diagonal elements of the diabatic Hamiltonian or (ii) forming a Hermitian dipole moment matrix based on the geometric mean of the components of the left and right transition dipole moment vectors and using eq 2 to calculate the electronic coupling. When the left and right transition dipole moments are not collinear, small differences can arise between these two approaches. We have used approach ii in all cases. Among the geometries considered here, only the H-bonded dimer presents a geometry for which the two transition dipole moments *could* be noncollinear, and a test calculation at a representative geometry showed the cosine of the angle between them to be 1 to better than five decimal places. No conclusions drawn below will be affected by the use of method ii.

The water dimer geometries considered are shown in Figure 1. The O−O distance in the dimers was taken as 2.8, 3.0, or 3.2 Å. The water geometry was taken from experiment[96] for the C_{2v}, C_{2v} H-bond, perp, and face (R_{OH} = 0.957 Å, θ_{HOH} = 104.5°) orientations. For the H-bonded dimer, our geometry is a model of the gas-phase equilibrium structure of the water dimer based on that of Frisch et al.[97] and quoted by Feller[98] (MP2 optimization in the 6-311++G(2d,2p) geometry, R_{OH} = 0.9571 Å, θ_{HOH} = 104.34°). We adjust the O−O distance to be 2.8, 3.0, or 3.2 Å for direct comparison with the other dimers studied here.

Using the above water dimer geometries, we add a pair of Be or Li along the O−O line of centers at D/A−nearest O distances of 2.5, 3.0, or 4.0 Å, as illustrated in Figure 2 for the C_{2v} H-bond geometry. These are referred to as "linear" geometries below. For an O−O distance of 2.8 Å and a Be−nearest O distance of 4.0 Å, the Be−Be separation is 10.8 Å. We also quote results from calculations based on the H-bonded dimer with Be atoms placed off the O−O line of centers. In these cases, we placed the Be atoms in positions to mimic the Be−water orientation in C_{2v} H-bond, perp, or a dimer with a Be along an O−H bond of each member of the dimer. In these cases, we also rotated one water about the O−O vector to avoid short Be−Be distances. In test calculations on the linear Be−H-bonded−Be^+ system, we found that rotation of one water

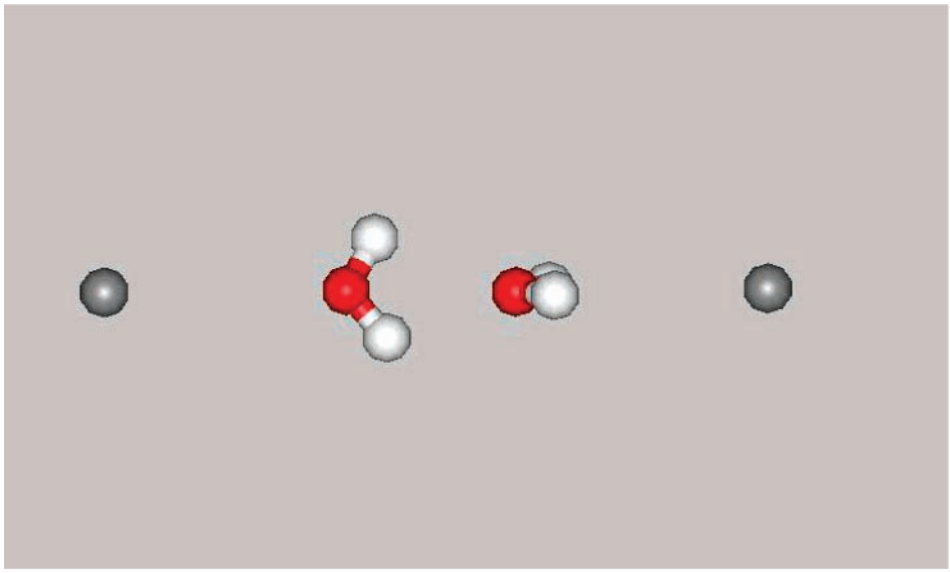

Figure 2. Geometry of linear Be−C_{2v} H-bond−Be$^+$.

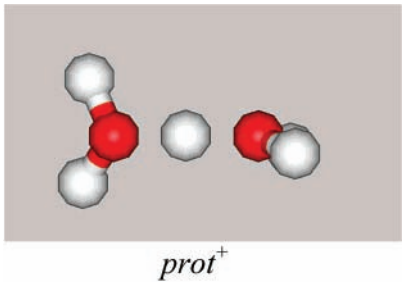

Figure 3. Model of prot$^+$ (i.e., $H_5O_2^+$).

about the O−O vector had less than a 1% effect on the coupling, and we expect this to be the case for the nonlinear cases as well.

Finally, we also examine the effects on D/A coupling with a protonated water dimer between D and A. A model of the protonated dimer (denoted prot$^+$) is shown in Figure 3, and the geometry used had C_2 symmetry (from an MP2 geometry optimization in the 6-311++G(2df,2pd) basis). The O−O distance is 2.382 Å, and the O−O distance was not varied in any of the calculations.

All EOM calculations were performed using ACES II.[99] The geometry optimization for the protonated water dimer was performed using Gaussian 98.[100]

III. Results

Values of H_{DA} for Be_2^+ with two intervening waters are presented in Tables 1−3. The intervening waters are oriented in the geometries noted in Figure 1 or in the geometry of the protonated dimer of Figure 3. In Tables 1 and 2, $R_{OO} = 2.8$ Å for the neutral dimers, whereas in Table 3, $R_{OO} = 3.2$ Å. In Tables 1 and 3, $R_{Be-O} = 4.0$ Å, and it is 3.0 Å in Table 2. Thus, in addition to examining different dimer orientations, these data also examine the sensitivity of the coupling to the O−O distance (over the range 2.8−3.2 Å) and the Be−O distance (over the range 3.0−4.0 Å).

The results of Tables 1 and 2 indicate that the H-bonded dimer orientation yields coupling elements comparable to, but not significantly larger than, those of other dimer orientations. The perp dimer produces the largest coupling elements for Be as D and A. The relative difference between the perp value and the next largest value is greater at $R_{BeBe} = 10.8$ Å than at 8.8 Å.

TABLE 1: H_{DA} for Be−[H_2O]$_2$−Be$^+$ and Be−[$H_5O_2^+$]−Be$^+$ for Various Geometries[a]

dimer	H_{DA} (eV)
C_{2v}	0.00235
C_{2v} H-bond	0.00342
perp	0.00663
face	0.00244
H-bonded	0.00365
prot$^+$ [b]	0.00483
no waters[c]	0.00006

[a] $R_{BeBe} = 10.8$ Å and $R_{OO} = 2.8$ Å for all neutral dimer geometries. [b] The Be−Be distance is 10.8 Å, and the dimer geometry is the optimized geometry with $R_{OO} = 2.382$ Å. [c] Be−Be distance of 10.8 Å with no waters. Be basis is the augmented 6-311G(d,p) basis set.

TABLE 2: H_{DA} for Be−[H_2O]$_2$−Be$^+$ and Be−[$H_5O_2^+$]−Be$^+$ for Various Geomtries[a]

dimer	H_{DA} (eV)
C_{2v}	0.0258
C_{2v} H-bond	0.0327
perp	0.0477
face	0.0283
H-bonded	0.0358
prot$^+$ [b]	0.0418
no waters[c]	0.00088

[a] $R_{BeBe} = 8.8$ Å and $R_{OO} = 2.8$ Å for all neutral dimer geometries. [b] The Be−Be distance is 8.8 Å, and the dimer geometry is the optimized geometry with $R_{OO} = 2.382$ Å. [c] Be−Be distance of 8.8 Å with no waters. The Be basis is the augmented 6-311G(d,p) basis set.

The C_{2v} H-bond dimer allows two nonlinear H-bonds in a symmetric arrangement, and the coupling element is similar to that for the H-bonded dimer. The prot$^+$ dimer produces coupling comparable to that of the unprotonated dimers. Similar results are obtained at the longer R_{OO} distance treated in Table 3. Variations on the C_{2v} structures with each water orientation reversed relative to the C_{2v} geometry or with one water rotated 90° about the Be−Be axis relative to the C_{2v} H-bond geometry were also examined and yielded similar values to those for the C_{2v} and C_{2v} H-bond dimers.

In any Be−[H_2O]$_2$−Be structure, three sets of orbital overlaps can be thought of as giving rise to the overall coupling. Crudely, the sets are left-Be/left-water, left-water/right-water, and right-water/right-Be. (Sequential coupling dominates for these weakly interacting cases.[89]) In choosing the various water dimer

TABLE 3: H_{DA} for Be−[H_2O]$_2$−Be^+ for Various Geometries[a]

dimer	H_{DA} (eV)
C_{2v}	0.00151
C_{2v} H-bond	0.00192
perp	0.00350
face	0.00141
H-bonded	0.00213
no waters[b]	0.00004

[a] $R_{BeBe} = 11.2$ Å and $R_{OO} = 3.2$ Å for all neutral dimer geometries. [b] Be−Be distance of 11.2 Å with no waters. Be basis is the augmented 6-311G(d,p) basis set.

TABLE 4: β Values for Be−[H_2O]$_2$−Be^+ and Be−[$H_5O_2^+$]−Be^+ for Variation of R_{BeBe} or R_{OO}[a]

dimer	β_{Be-Be} (Å^{-1})[b]	β_{O-O} (Å^{-1})[c]
C_{2v}	2.3	2.2
C_{2v} H-bond	2.1	2.9
perp	1.7	3.2
face	2.35	2.7
H-bonded	2.1	2.7
$prot^+$	2.1	

[a] Dimer indicates the water dimer geometry. β is determined by a fit of the equation $\ln(H_{DA}) =$ constant $- (\beta/2)R$. [b] $R_{OO} = 2.8$ Å for neutral dimers and 2.379 Å for the protonated dimer; R_{BeBe} values in the fit were 7.8, 8.8, and 10.8 Å. [c] $R_{BeO} = 4.0$ Å, and R_{OO} values in the fit were 2.8, 3.0, and 3.2 Å.

geometries in Tables 1−3, with fixed Be positions, we change all three types of overlaps, and it might be suggested that unfavorable Be−water overlap is what is giving rise to the comparable H-bonded and non-H-bonded dimer (e.g., C_{2v}, C_{2v} H-bond, perp, face) couplings obtained here. We investigated this by fixing the H-bonded dimer distance ($R_{OO} = 2.8$ Å) while placing the Be atoms at positions that would mimic the Be−water overlap obtained in (i) the C_{2v} H-bond dimer, (ii) the perp dimer, and (iii) a dimer with Be atoms placed along O−H bonds on each end of the H-bonded dimer structure. The Be atoms were 4 Å from their nearest O atoms, and the H-bond-donating water was rotated about the O−O axis to yield Be−Be distances greater than 8.5 Å (to avoid significant direct coupling). These models thus mimic the nearest-neighbor distances in the 10.8/2.8 structures, (i.e., the geometries of Table 1). Using the 6-311G(d,p) basis, the coupling elements for these three structures were 0.0026, 0.0038, and 0.0028 eV, respectively, whereas the linear dimer coupling element in this basis was 0.0038 eV. Thus, the coupling through the H-bonded dimer is not significantly affected by the position of the Be atoms.

In Table 4 values of β are presented for water-dimer-mediated coupling assuming that H_{DA} decays as

$$H_{DA} = A \exp(-\beta R_{DA}/2) \tag{3}$$

with distance. Modest departure from a purely exponential distance dependence is observed here, especially at the shorter Be−O distances. However, for purposes of comparison between the various dimer orientations, this paramertization should be adequate. The data for variation of R_{BeBe} values fixes the water dimer R_{OO} distance while the Be−Be distance is increased. However, when R_{OO} is varied, the Be−Be distance is increased in concert with the O−O distance. The β values are distinct for these two distance variations, with the O−O dependence generally being steeper (larger β) than the Be−Be dependence. The β values for the Be−Be distance variation are lower than those obtained with no water present (2.71 Å^{-1}),[62] whereas those obtained on the basis of O−O distance changes are generally

TABLE 5: H_{DA} for Li−[H_2O]$_2$−Li^+ and Li−[$H_5O_2^+$]−Li^+ for Various Geometries[a]

dimer	H_{DA} (eV)
C_{2v}	0.0135
C_{2v} H-bond	0.0145
perp	0.0126
face	0.0182
H-bonded	0.0135
$prot^+$ [b]	0.1084
no waters[c]	0.00362

[a] $R_{LiLi} = 10.8$ Å and $R_{OO} = 2.8$ Å for all neutral dimer geometries. [b] The Li−Li distance is 10.8 Å, and the dimer geometry is the optimized geometry with $R_{OO} = 2.382$ Å. [c] Li−Li distance of 10.8 Å with no waters. The Li basis is the augmented 6-311G(d,p) basis set.

TABLE 6: β Values for Li−[H_2O]$_2$−Li^+ and Li−[$H_5O_2^+$]−Li^+ for Variations of R_{LiLi} or R_{OO}[a]

dimer	β_{Li-Li} (Å^{-1})[b]	β_{O-O} (Å^{-1})[c]
C_{2v}	1.8	1.3
C_{2v} H-bond	1.9	1.6
perp	1.6	1.9
face	1.5	1.7
H-bonded	1.4	1.8
$prot^+$	0.70	

[a] Dimer indicates the water dimer geometry. β is determined by a fit of the equation $\ln(H_{DA}) =$ constant $- (\beta/2)R$. [b] $R_{OO} = 2.8$ Å for the neutral dimers and 2.379 Å for the protonated dimer; R_{LiLi} values in the fit were 7.8, 8.8, and 10.8 Å. [c] $R_{LiO} = 4.0$ Å and R_{OO} values in the fit were 2.8, 3.0, and 3.2 Å.

equal to or greater than those obtained with no waters present. At short distances, one would not expect β to be equal in these two cases, as its size is governed, in a superexchange picture, by the changing overlap of different localized states for the two geometry changes (Be−water in the Be−Be case, water−water in the O−O case). At larger separations, however, these β values will become equal since the long-range behavior of the states will be governed by the ionization potentials corresponding to the highest-lying ion states. The O−O distance dependence is strongest for perp, which exhibited the largest values for the coupling element in Tables 1−3.

Analogous results are presented for Li as D and A in Tables 5 and 6. The H_{DA} values in Table 5 for the neutral dimers show even less variation than was observed in the Be case; for Li as donor and acceptor, the water dimer geometry has essentially no effect on the coupling. Water nevertheless is important in mediating the coupling since comparison of the dimer-mediated coupling with that for Li_2^+ with no waters present indicates that the coupling is enhanced by the presence of the waters. The protonated dimer yields a dramatic increase in the coupling element compared to those obtained for the neutral dimers. We argue below that the difference in protonated dimer results between Be and Li as D/A arises from different superexchange mechanisms in the two cases (i.e., hole transfer for Be and particle transfer for Li).

The β values for Li as D/A (Table 6) are lower than those obtained with Be. Since Li has a lower IP, one expects slower orbital decay with distance[66] and thus smaller β values as the D−A distance is changed. We find that the dependence of the coupling on the O−O distance is also weaker for Li than for Be.

We compared the GMH charge-transfer distance (based on the diabatic dipole moment difference) with the actual value of R_{BeBe} and found the former to be shorter by up to 1 Å at $R_{BeBe} = 7.8$ Å and by up to 0.5 Å at the larger R_{BeBe}. This is consistent with a small amount of rehybridization/delocaliza-

TABLE 7: Comparison of Ionization Potentials (eV)[a]

parentage	Be_2	H_2O	Be−face−Be	Be−perp−Be
Be/2s	8.40/9.28, 8.40/9.28		9.35, 9.36	9.09, 9.10
water/$1b_1$		13.6/12.0	11.8, 12.1	11.1, 12.4
water/$3a_1$		15.6/14.3	14.0, 14.5	13.9, 14.2
water/$1b_2$		19.2/18.7	17.5, 19.8	18.3, 18.5
water/$2a_1$		36.5/32.3		

[a] Ionization potentials for various systems, grouped according to parentage of the state relative to isolated Be or water. For Be_2 and H_2O, the first entry is the Koopmanns' estimate, and the second is the EOM-IP estimate. For all Be−dimer−Be clusters, only the EOM-IP estimate is reported, at the 10.8/2.8 geometry in each case. The Be−Be distance in Be_2 is 10.8 Å. Multiple entries indicate pairs of orbitals arising from the atomic/molecular parent.

tion (the ^{1}P states of Be are 5.5 eV above the ground state, whereas the ^{2}P states of Be^+ are 4 eV above its ^{2}S ground state), but the charge-transfer distance did not correlate in any significant way with the variation of the coupling with dimer geometry at a given distance. For Li as donor/acceptor with the neutral dimers as the bridge, the CT distances were shorter than the actual R_{LiLi} distances by up to 1.7 Å at $R_{LiLi} = 7.8$ Å, with much closer agreement (within 1 Å) at larger distances. For comparison, with no intervening waters, the GMH CT distance is 7.6 Å (6.9 Å) for Be_2^+ (Li_2^+) at 7.8 Å separation, showing smaller but similar rehybridization effects than those seen with waters present. However, the protonated dimer charge-transfer distances with Li_2^+ as the D/A pair are considerably shorter (nearly 3 Å shorter for $R_{LiLi} = 7.8-10.8$ Å) than the actual R_{LiLi}, suggesting that significant delocalization and rehybridization are occurring. (The ^{2}P states of Li are only 1.8 eV above the ^{2}S ground state in this basis.) To that extent, the protonated results may represent somewhat different initial and final diabatic states than the nonprotonated dimers, thus making direct comparison somewhat more difficult. However, they may also reflect very real effects due to protonation on high-energy (e.g., excited-state) et and thus are presented here.

Whereas most water dimer geometries yield comparable coupling values for a given D/A pair, the two unusual cases in the present results are Be−perp−Be^+ and Li−$prot^+$−Li^+, each of which produces coupling elements dramatically larger than the other water dimer geometries considered. In a superexchange model,[9,26] one expects the coupling to depend on (i) the electronic coupling elements connecting various sites and (ii) the energy differences between D/A and bridge ion states. In these two unusual cases, site−site electronic coupling plays a role in determining the relative couplings. However, it is not the sole reason for the unusually high coupling since identical donor−dimer−acceptor orientations are present in Li−perp−Li^+ and Be−$prot^+$−Be^+ and their couplings are comparable to those observed for the other dimer geometries. It turns out that near-degeneracy effects also play an important role in these two cases for distinct reasons.

Consider Be−perp−Be^+ first. In Table 7, we compare ionization potentials (IPs) for Be_2, water, and two Be−dimer−Be systems (perp and face). The Be parentage states are associated with many-electron states of the form Be^+−dimer−Be, whereas the water parentage states are associated with states of the form Be−$dimer^+$−Be. Comparison of the two sets of Be−dimer−Be IPs with each other and with those for a single water indicates a good deal of similarity. The water orbital IPs for the dimers can be associated easily with the single-water states. However, closer inspection reveals that in the perp dimer the highest IP is almost 1 eV higher than that for a single water, whereas in the face dimer, the highest IP is only 0.2 eV higher than for a single water. These states correspond to ionization from the water b_1 orbital, the p orbital perpendicular to the molecular plane. The lower IP in the perp dimer arises because these p orbitals lie along the same line in the perp orientation, and at short distances, they overlap considerably, giving rise to a strong interaction. (This effect is diminished somewhat as the O−O distance is increased (Table 3)). The perp geometry thus leads to a significant decrease in the energy of the highest $bridge^+$ state relative to that of the D/A states, and on a superexchange basis, one would expect a larger contribution from these states to the coupling. This does not occur in the other dimer geometries since the $bridge^+$ states are not lowered as much in these geometries (see Table 7), and in the C_{2v}, C_{2v} H-bond, and face geometries, these b_1 ion states are symmetry-forbidden from contributing to the coupling.

Thus, in the case of Be−perp−Be^+, we believe the enhanced hole-mediated coupling originates from a combination of (i) lowered energy of $dimer^+$ states relative to D/A^+ peculiar to the perp geometry, (ii) symmetry-allowed interaction with these low-energy $dimer^+$ states in the perp geometry, and (iii) the high IP of Be in comparison with that of Li. Note that factors i and ii are obtained in the Li−perp−Li^+ case as well, but its coupling is not enhanced because the Li IP (5.35 eV) is still well removed from the highest $perp^+$ state.

In the case of Li−$prot^+$−Li^+, we suggest a related explanation that is now based on the energetic proximity to particle-like states of the bridge (i.e., Li^+−$prot^0$−Li^+ states). Protonation of the water dimer stabilizes hole- and particle-like states of the bridge. Given the low IP of Li, the hole-like states are moved farther from the Li−$prot^+$−Li^+ initial and final states, whereas the particle-like states are significantly closer in energy to the initial and final states (within 3 eV), and strong mixing occurs. The evidence of greater delocalization noted above supports this explanation but also suggests that some of the enhancement in the coupling may stem from somewhat more delocalized initial and final diabatic states. Be's higher IP limits this mixing with the particle-like states, and thus the coupling in Be−$prot^+$−Be^+ is not enhanced significantly relative to that of the unprotonated dimer.

The many-electron treatment used here does not allow a simple factorization into hole- and particle-mediated pathways, thus it is not possible in general to specify which is operative in each dimer geometry considered here. However, the relative energetics of the systems coupled with the unusual behavior of Li−$prot^+$−Li^+ and Be−perp−Be^+ suggest that tunneling through water for Li may be dominated by particle transfer, whereas that for Be may be dominated by hole-transfer contributions.

In passing, we note that a comparison of the Koopman's theorem and EOM-IP results (Table 7) for Be_2 and water indicates that electron correlation plays an important role in obtaining accurate relative energetics for these systems. Correlation increases the IP of Be and lowers the IP for water relative to the Koopman's theorem estimates. Although correlation will not always play such a dramatic role, in the perp geometry, we find that SCF coupling elements are half those of the EOM-IP results.

IV. Discussion

The above results indicate that, at comparable distances, H-bonded and non-H-bonded water dimer geometries produce similar values of the electronic coupling element for D/A pairs (within a factor of 1.5). This result is independent of D/A energy. That the coupling calculated with waters present is due largely to superexchange interactions is demonstrated by the much

smaller couplings obtained for direct (i.e., no waters present) coupling at equivalent D/A distances. Thus, at a *fixed* O−O distance, it appears that the presence or absence of an H-bond does not play a significant role in determining the electronic coupling for water dimers.

It is important to stress what our results say and do not say about H-bonds and the electronic coupling. First, they do not suggest that H-bonds are unimportant in mediating the electronic coupling between a donor and acceptor. The importance of H-bonds in mediating the electronic coupling has been clearly demonstrated in past experimental and theoretical studies.[14,70,75−81] Our previous studies of water-mediated electron transfer support this as well, given the comparable abilities of water−water orientations to mediate the coupling.[62,89] Rather, the present results suggest that weak interactions, in general, have the ability to play a considerable role in mediating the electronic coupling.

Second, the present results emphasize comparisons at fixed distances between waters. They do not directly relate to couplings calculated at points of equal energy for the various dimer orientations. The energies (kcal/mole) of the Be−dimer−Be structures in the 10.8/2.8 geometries relative to that of the C_{2v} H-bond structure are 16.1, 0, 9.6, 16.8, and −1.4 for the C_{2v}, C_{2v} H-bond, perp, face, and H-bonded dimers, respectively. At the 11.2/3.2 geometries, the relative energies are 8.7, 0, 6.8, 10.2, and −1.0. (Using a simple dipole−dipole electrostatic interaction model with a 3.2-Å separation and the CCSD dipole moment for water in this basis (2.15 D), the relative energies of the C_{2v}, C_{2v} H-bond, perp, and face water dimers are 8.2, 0, 6.1, and 6.1 kcal/mol, respectively. Differences between the electrostatic and the actual values become more pronounced at 2.8 Å and can be attributed to weak Be−water interactions, overlap effects, and deviations from simple dipole−dipole interactions. The latter arises especially for the C_{2v} and face geometries, where H atoms are in closer contact than for other geometries.) Were one to compare the coupling for the C_{2v}, perp, face, and C_{2v} H-bond geometries, at comparable total energies to the H-bonded dimer geometry the O−O distances would be considerably larger, leading to smaller couplings relative to the H-bonded configuration. However, in a protein or condensed phase, packing may force van der Waals contacts of non-H-bonded atoms situated between the donor and acceptor. Our results suggest that these contacts may play a larger role in mediating the coupling than has been suggested previously.[2]

Third, the results do not indicate that *all* weak interactions will yield couplings comparable to *all* H-bonds. Energetic and overlap considerations will undoubtedly play a significant role in determining the relative strengths of weak-interaction-mediated couplings. Thus, the present results do not provide support for global assertions about the electronic coupling mediated by weak interactions.

However, the present results do suggest that it may be worthwhile to reevaluate the relative sizes of H-bonded and non-H-bonded interactions for condensed-phase electron transfers relative to the Pathway Model estimates.[2] The Pathway Model was developed as a means of broadly assessing distance dependence in protein-mediated electron transfers. It would be unrealistic to expect quantitative accuracy of the model in general, and no such claims have been made. The present results suggest that the parametrization of the coupling mediated by non-H bonded weak interactions (through-space jumps in the pathway model) *may* lead to an underestimate of their importance in some cases.

We also note that the β values obtained for O−O distance changes are strongly dependent on D/A energy (see Tables 4 and 6). Although we consider only ground-state transfers here, the low IP of Li places its energy near that of what one might expect for photoexcited donors and acceptors in many systems. Our results suggest that excited-state transfers may be more sensitive to the protonation state within the bridging medium, perhaps even to the point of promotion of a hopping-type mechanism for charge transport. Further work is required to address this in detail.

V. Conclusions

The present results suggest that weak interactions have the potential to play a significant role in mediating the electronic coupling. Using water dimers as bridges between atomic donors and acceptors, we have shown that a variety of dimer geometries, none of which possesses a conventional H-bond, yield D/A couplings comparable to and sometimes greater than the H-bonded water dimer. We find that protonation of the water dimer has a dramatic effect on the D/A coupling only for relatively high-energy D/A states. The decay with distance of the coupling is examined, and only minor differences between H-bonded and non-H-bonded cases are observed. However, the decay is strongly affected by D/A energy. These results suggest that further investigation is warranted of the role of weak interactions in mediating the electronic coupling in condensed-phase electron transfers.

Acknowledgment. We acknowledge financial support from the National Science Foundation (CHE-9731634) and the donors of the Petroleum Research Fund. R.J.C. gratefully acknowledges a grant from the Rutgers University Nanochemistry Consortium.

References and Notes

(1) Gray, H. B.; Winkler, J. R. *Annu. Rev. Biochem.* **1996**, *35*, 537.
(2) Onuchic, J. N.; Beratan, D. N.; Winkler, J. R.; Gray, H. B. *Annu. Rev. Biophys. Biomol. Struct.* **1992**, *21*, 349.
(3) Ponce, A.; Winkler, J. R.; Gray, H. B. *J. Am. Chem. Soc.* **2000**, *122*, 8187.
(4) Tezcan, F. A.; Crane, B. R.; Winkler, J. R.; Gray, H. B. *Proc. Natl. Acad. Sci. U.S.A.* **2001**, *98*, 5002.
(5) Winkler, J. R.; Di Bilio, A. J.; Farrow, N. A.; Richards, J. H.; Gray, H. B. *Pure Appl. Chem.* **1999**, *71*, 1753.
(6) Newton, M. D.; Sutin, N. *Annu. Rev. Phys. Chem.* **1985**, *35*, 437.
(7) Newton, M. D. Control of Electron-Transfer Kinetics: Models for Medium Reorganization and Donor−Acceptor Coupling. In *Electron Transfer—From Isolated Molecules to Biomolecules*; Jortner, J., Bixon, M., Eds.; Advances in Chemical Physics; John Wiley: New York, 1999; Vol 106, Pt 1, p 303.
(8) Newton, M. D.; Cave, R. J. Molecular Control of Electorn and Hole Transfer Processes: Theory and Applications. In *Molecular Electronics*; Jortner, J., Ratner, M., Eds.; Blackwell: Malden, MA, 1997.
(9) Newton, M. D. *Chem. Rev.* **1991**, *91*, 767.
(10) Onuchic, J. N.; Beratan, D. N. *J. Chem. Phys.* **1990**, *92*, 722.
(11) Skourtis, S. S.; Beratan, D. N. Theories of Structure−Function Relationships for Bridge-Mediated Electron-Transfer Reactions. In *Electron Transfer—From Isolated Molecules to Biomolecules*; Jortner, J., Bixon, M., Eds.; Advances in Chemical Physics; John Wiley: New York, 1999; Vol 106, Pt 1, p 377.
(12) Tong, G. S. M.; Kurnikov, I. V.; Beratan, D. N. *J. Phys. Chem. B* **2002**, *106*, 2381.
(13) Beratan, D. N.; Priyadarshy, S.; Risser, S. M. *Chem. Biol.* **1997**, *4*, 3.
(14) Medvedev, D. M.; Daizadeh, I.; Stuchebrukhov, A. A. *J. Am. Chem. Soc.* **2000**, *122*, 6571.
(15) Stuchebrukhov, A. A.; Song, X. Y. *J. Chem. Phys.* **1994**, *101*, 9354.
(16) Stuchebrukhov, A. A.; Marcus, R. A. *J. Phys. Chem.* **1995**, *99*, 7581.
(17) Stuchebrukhov, A. A. *Int. J. Quantum Chem.* **2000**, *77*, 16.
(18) Isied, S. *Adv. Chem. Ser.* **1997**, *253*, 331.
(19) Marcus, R. A. *J. Chem. Phys.* **1965**, *43*, 679.
(20) Marcus, R. A.; Sutin, N. *Biochim. Biophys. Acta* **1985**, *811*, 265.
(21) Levich, V. G. *Adv. Electrochem. Electrochem. Eng.* **1966**, *4*, 249.
(22) Dogonadze, R. R.; Kuznetsov, A. M.; Vorotyntsev. *Phys. Status Solidi B* **1972**, *54*, 125.

(23) Hush, N. S. *Trans. Faraday Soc.* **1961**, *57*, 557.
(24) Hush, N. S. *Electrochim. Acta* **1968**, *13*, 1005.
(25) Kestner, N. R.; Logan, J.; Jortner, J. *J. Phys. Chem.* **1974**, *78*, 2148.
(26) McConnell, H. M. *J. Chem. Phys.* **1961**, *35*, 508.
(27) Halpern, J.; Orgel, L. E. *Discuss. Faraday Soc.* **1960**, *29*, 32.
(28) Beratan, D. N.; Hopfield, J. J. *J. Am. Chem. Soc.* **1984**, *106*, 1584.
(29) Beratan, D. N.; Onuchic, J. N.; Hopfield, J. J. *J. Phys. Chem.* **1986**, *90*, 3707.
(30) Kurnikov, I. V.; Beratan, D. N. *Abstr. Pap. − Am. Chem. Soc.* **1995**, *210*, 119.
(31) Kurnikov, I. V.; Beratan, D. N. *J. Chem. Phys.* **1996**, *105*, 9561.
(32) Priyadarshy, S.; Beratan, D. N.; Risser, S. M. *Int. J. Quantum Chem.* **1996**, *60*, 65.
(33) Skourtis, S. S.; Onuchic, J. N.; Beratan, D. N. *Inorg. Chim. Acta* **1996**, *243*, 167.
(34) Liang, C.; Newton, M. D. *J. Phys. Chem.* **1992**, *96*, 2855.
(35) Liang, C.; Newton, M. D. *J. Phys. Chem.* **1992**, *97*, 3199.
(36) Logan, J.; Newton, M. D. *J. Chem. Phys.* **1983**, *1983*, 4086.
(37) Newton, M. D. *J. Phys. Chem.* **1991**, *95*, 30.
(38) Newton, M. D.; Ohta, K.; Zhing, E. *J. Phys. Chem.* **1991**, *95*, 2317.
(39) Smalley, J. F.; Feldberg, S. W.; Chidsey, C. E. D.; Linford, M. R.; Newton, M. D.; Liu, Y. P. *J. Phys. Chem.* **1995**, *99*, 13141.
(40) Cheung, M. S.; Daizadeh, I.; Stuchebrukhov, A. A.; Heelis, P. F. *Biophys. J.* **1999**, *76*, 1241.
(41) Daizadeh, I.; Medvedev, E. S.; Stuchebrukhov, A. A. *Proc. Natl. Acad. Sci. U.S.A.* **1997**, *94*, 3703.
(42) Daizadeh, I.; Gehlen, J. N.; Stuchebrukhov, A. A. *J. Chem. Phys.* **1997**, *106*, 5658.
(43) Daizadeh, I.; Medvedev, D. M.; Stuchebrukhov, A. A. *Mol. Biol. Evol.* **2002**, *19*, 406.
(44) Gehlen, J. N.; Daizadeh, I.; Stuchebrukhov, A. A.; Marcus, R. A. *Inorg. Chim. Acta* **1996**, *243*, 271.
(45) Medvedev, E. S.; Stuchebrukhov, A. A. *Pure Appl. Chem.* **1998**, *70*, 2201.
(46) Stuchebrukhov, A. A. *J. Chem. Phys.* **1996**, *105*, 10819.
(47) Stuchebrukhov, A. A. *J. Chem. Phys.* **1996**, *104*, 8424.
(48) Stuchebrukhov, A. A. *J. Chem. Phys.* **1997**, *107*, 6495.
(49) Stuchebrukhov, A. A. *Abstr. Pap. − Am. Chem. Soc.* **1998**, *216*, 393.
(50) Siddarth, P.; Marcus, R. A. *J. Phys. Chem.* **1992**, *96*, 3213.
(51) Siddarth, P.; Marcus, R. A. *J. Phys. Chem.* **1993**, *97*, 13078.
(52) Braga, M.; Broo, A.; Larsson, S. *Chem. Phys.* **1991**, *156*, 1.
(53) Braga, M.; Larsson, S. *J. Phys. Chem.* **1993**, *97*, 8929.
(54) Broo, A.; Larsson, S. *J. Phys. Chem.* **1991**, *95*, 4925.
(55) Larsson, S.; Rodriguez-Monge, L. *Int. J. Quantum Chem.* **1996**, *58*, 517.
(56) Larsson, S. *J. Phys. Chem.* **1984**, *88*, 1321.
(57) Larsson, S.; Klimkans, A. *J. Mol. Struct.: THEOCHEM* **1999**, *464*, 59.
(58) Rodriguezmonge, L.; Larsson, S. *J. Chem. Phys.* **1995**, *102*, 7106.
(59) Curtiss, L. A.; Naleway, C. A.; Miller, J. R. *J. Phys. Chem.* **1993**, *97*, 4050.
(60) Curtiss, L. A.; Naleway, C. A.; Miller, J. R. *J. Phys. Chem.* **1995**, *99*, 1182.
(61) Curtiss, L. A.; Miller, J. R. *J. Phys. Chem. A* **1998**, *102*, 160.
(62) Miller, N. E.; Wander, M. C.; Cave, R. J. *J. Phys. Chem. A* **1999**, *103*, 1084.
(63) Paulson, B. P.; Curtiss, L. A.; Bal, B.; Closs, G. L.; Miller, J. R. *J. Am. Chem. Soc.* **1996**, *118*, 378.
(64) Cave, R. J.; Newton, M. D. *J. Chem. Phys.* **1997**, *106*, 9213.
(65) Cave, R. J.; Newton, M. D.; Kumar, K.; Zimmt, M. B. *J. Phys. Chem.* **1995**, *99*, 17501.
(66) Cave, R. J.; Baxter, D. V.; Goddard, W. A. I.; Baldeschwieler, J. D. *J. Chem. Phys.* **1987**, *87*, 926.
(67) Farazdel, A.; Dupuis, M.; Clementi, E.; Aviram, A. *J. Am. Chem. Soc.* **1990**, *112*, 4206.
(68) Jordan, K. D.; Nachtigallova, D.; Paddon-Row, M. N. Long-Range Intramolecular Interactions: Implications for Electron Transfer. In *Modern Electronic Structure Theory and Applications in Organic Chemistry*; Davidson, E. R., Ed.; World Scientific: River Edge, NJ, 1997; p 257.
(69) Paddon-Row, M. N.; Wong, S. S.; Jordan, K. D. *J. Am. Chem. Soc.* **1990**, *112*, 1710.
(70) Zhao, X. G.; Cukier, R. I. *J. Phys. Chem.* **1995**, *99*, 645.
(71) Cukier, R. I.; Nocera, D. G. *Annu. Rev. Phys. Chem.* **1998**, *49*, 337.
(72) Hammes-Schiffer, S. *Acc. Chem. Res.* **2001**, *34*, 273.
(73) Kobrak, M. N.; Hammes-Schiffer, S. *J. Phys. Chem. B* **2001**, *105*, 10435.
(74) Rege, P. J.; Williams, S. A.; Therien, M. J. *Science (Washington, D.C.)* **1995**, *269*, 1409.
(75) Williamson, D. A.; Bowler, B. E. *J. Am. Chem. Soc.* **1998**, *120*, 10902.
(76) Yang, J.; Seneviratne, D.; Arbatin, G.; Andersson, A. M.; Curtis, J. C. *J. Am. Chem. Soc.* **1997**, *119*, 5329.
(77) Osuka, A.; Yoneshima, R.; Shiratori, H.; Okada, T.; Taniguchi, S.; Mataga, N. *Chem. Commun.* 1567.
(78) Sessler, J. L.; Satiosatham, M.; Brown, C. T.; Rhodes, T. A.; Wiederrecht, G. *J. Am. Chem. Soc.* **2001**, *123*, 3655.
(79) Ghaddar, T. H.; Castner, E. W.; Isied, S. *J. Am. Chem. Soc.* **2000**, *122*, 1233.
(80) Antony, J.; Medvedev, D. M.; Stuchebrukhov, A. A. *J. Am. Chem. Soc.* **2000**, *122*, 1057.
(81) Newton, M. D. *J. Electroanal. Chem.* **1997**, *438*, 3.
(82) Ghanty, T. K.; Staroverov, V. N.; Koren, P. R.; Davidson, E. R. *J. Am. Chem. Soc.* **2000**, *122*, 1210.
(83) Napper, A. M.; Read, I.; Waldeck, D. H.; Head, N. J.; Oliver, A. M.; Paddon-Row, M. N. *J. Am. Chem. Soc.* **2000**, *122*, 5220.
(84) Kumar, K.; Kurnikov, I. V.; Beratan, D. N.; Waldeck, D. H.; Zimmt, M. B. *J. Phys. Chem. A* **1998**, *102*, 5529.
(85) Krishnan, R.; Binkley, J. S.; Seeger, R.; Pople, J. A. *J. Chem. Phys.* **1980**, *72*, 650.
(86) Clark, T.; Chandrasekhar, J.; Sptiznagel, G. W.; Schleyer, P. v. R. *J. Comput. Chem.* **1983**, *4*, 294.
(87) Cave, R. J.; Newton, M. D. *Chem. Phys. Lett.* **1996**, *249*, 15.
(88) Rust, M.; Lappe, J.; Cave, R. J. *J. Phys. Chem. A* **2002**, *106*, 3930.
(89) Henderson, T. M.; Cave, R. J. *J. Chem. Phys.* **1998**, *109*, 7414.
(90) Bartlett, R. J.; Stanton, J. F. Applications of Post-Hartree−Fock Methods: A Tutorial. In *Reviews in Computational Chemistry*; Lipkowitz, K. B., Boyd, D. B., Eds.; VCH: New York, 1994; Vol 5, p 65.
(91) Stanton, J. F.; Bartlett, R. J. *J. Chem. Phys.* **1993**, *98*, 7029.
(92) Watts, J. D.; Gwaltney, S. R.; Bartlett, R. J. *J. Chem. Phys.* **1996**, *105*, 6979.
(93) Stanton, J. F.; Sattelmeyer, K. W.; Gauss, J.; Allan, M.; Skalicky, T.; Bally, T. *J. Chem. Phys.* **2001**, *115*, 1.
(94) Nooijen, M.; Bartlett, R. J. *J. Chem. Phys.* **1995**, *102*, 6735.
(95) Nooijen, M.; Bartlett, R. J. *J. Chem. Phys.* **1995**, *102*, 3629.
(96) Benedict, W. S.; Gailer, N.; Pyler, E. K. *J. Chem. Phys.* **1956**, *24*, 1139.
(97) Frisch, M. J.; DelBene, J. E.; Binkley, J. S.; Schaefer, H. F. I. *J. Chem. Phys.* **1986**, *84*, 2279.
(98) Feller, D. *J. Chem. Phys.* **1992**, *96*, 6104.
(99) Stanton, J. F.; Gauss, J.; Watts, J. D.; Nooijen, M.; Oliphant, N.; Perera, S. A.; Szalay, P. G.; Lauderdale, W. J.; Kucharski, S. A.; Gwaltney, S. R.; Beck, S.; Balková, A.; Bernholdt, D. E.; Baeck, K. K.; Rozyczko, P.; Sekino, H.; Hober, C.; Bartlett, R. J. *Aces II*; Quantum Theory Project: Gainesville, FL, 1999.
(100) Frisch, M. J.; Trucks, G. W.; Schlegel, H. B.; Scuseria, G. E.; Robb, M. A.; Cheeseman, J. R.; Zakrzewski, V. G.; Montgomery, J. A., Jr.; Stratmann, R. E.; Burant, J. C.; Dapprich, S.; Millam, J. M.; Daniels, A. D.; Kudin, K. N.; Strain, M. C.; Farkas, O.; Tomasi, J.; Barone, V.; Cossi, M.; Cammi, R.; Mennucci, B.; Pomelli, C.; Adamo, C.; Clifford, S.; Ochterski, J.; Petersson, G. A.; Ayala, P. Y.; Cui, Q.; Morokuma, K.; Malick, D. K.; Rabuck, A. D.; Raghavachari, K.; Foresman, J. B.; Cioslowski, J.; Ortiz, J. V.; Stefanov, B. B.; Liu, G.; Liashenko, A.; Piskorz, P.; Komaromi, I.; Gomperts, R.; Martin, R. L.; Fox, D. J.; Keith, T.; Al-Laham, M. A.; Peng, C. Y.; Nanayakkara, A.; Gonzalez, C.; Challacombe, M.; Gill, P. M. W.; Johnson, B. G.; Chen, W.; Wong, M. W.; Andres, J. L.; Head-Gordon, M.; Replogle, E. S.; Pople, J. A. *Gaussian 98*, revision A.11.3; Gaussian, Inc.: Pittsburgh, PA, 1998.